State of the Art Thermal Barrier Coating (TBC) Materials and TBC Failure Mechanisms

Abdullah Cahit Karaoglanli, Kadir Mert Doleker and Yasin Ozgurluk

Abstract Thermal barrier coatings (TBCs) are widely used in the aviation industry to improve the service life of components being exposed to high temperatures. Providing a higher resistance compared to conventional coatings, TBCs also improve the performance and lifetime of materials through their thermal insulating characteristic. Resistance of gas turbine components, particularly turbine blades, vanes and combustion chambers, is required to be improved against failures such as corrosion, oxidation and thermal shock as well, since turbine inlet temperatures should be increased to improve the performance of gas turbine engines. Accordingly, it is aimed to obtain a better resistance and durability against the failure mechanisms through enhancement of the methods and materials used in thermal barrier coatings. In this study, thermal barrier coatings used in gas turbines as well as their structure, also the relevant failure mechanisms and the new material groups used in TBCs are discussed.

Keywords Thermal barrier coating (TBC) · Gas turbine · Failure mechanism · Advanced materials

1 Introduction to TBCs

TBCs are commonly used in high-temperature applications of aircrafts, gas turbines and advanced aero engine components like turbine pales, combustion chambers and nozzle vanes in order to increase efficiency and durability properties of these

A.C. Karaoglanli (✉) · K.M. Doleker · Y. Ozgurluk
Metallurgical and Materials Engineering Department, Bartin University,
74100 Bartin, Turkey
e-mail: cahitkaraoglanli@gmail.com

K.M. Doleker
e-mail: kmdoleker@bartin.edu.tr

Y. Ozgurluk
e-mail: yozgurluk@bartin.edu.tr

A. Öchsner and H. Altenbach (eds.), *Properties and Characterization of Modern Materials*, Advanced Structured Materials 33,
DOI 10.1007/978-981-10-1602-8_34

components [1–4]. The most important goal in using of TBCs is to reach a higher turbine inlet temperature and providing better propulsion [5, 6]. The aircraft turbine blade temperature, which is uncoated, goes up to approximately 1300 °C during running. Most of the metals do not remain at stable structure in this temperature range although air cooling systems are used [7]. Inconel alloys belonging to a type of the Ni based superalloys with respect to their superior mechanical properties are most suitable materials against high temperature conditions. However, they cannot preserve their structures under working conditions of gas turbines. Therefore, thermal barrier coated superalloys are using in this field [8]. A typical TBC consists of four diverse layers (i) a Ni based single crystal superalloy as substrate material, (ii) a metallic inner layer (bond coat) as MCrAlY (M=Ni,Co or both of them along with Fe), (iii) thermally grown oxide (TGO), (iv) a ceramic top coat [9–11].

The bond coat has the most critical role in TBC systems. MCrAlY coated above substrate material as bond coat provides a good adherence between the substrate material and top coat as well as oxidation resistance and tolerating thermal expansion mismatch [12]. Bond coats can be produced a in variety of methods such as atmospheric plasma spray (APS), vacuum plasma spray (VPS) or low pressure plasma spray (LPPS), cold gas dynamic spray (CGDS), high velocity oxy-fuel (HVOF) and electro-beam physical vapour deposition (EB-PVD). VPS is the best method to produce low oxide scales but it is more expensive compared to other methods [13]. HVOF and CGDS have optimum properties as characteristic and almost similar compared with one another while the APS method is the most economic production method, including higher oxide scale and porosity due to open air atmospheric production [14].

TGO is formed during the deposition, approximately 0.5–1 μm sizes but starting to grow due to high temperature oxidation and leading to spallation of the top coat from the bond coat. In TBCs, spallation arising from TGO is observed as the most common failure. Thus, a great amount of studies are done about this phenomenon [15–17]. Top coats used as ceramic based material are the last layer of the TBC system. The top coat provides thermal barrier due to being a ceramic based material which insulates the system against thermal effects and preserving stability. Thus, turbine inlet temperatures can be decreased in the range of 100 and 300 °C [7]. There are two types of methods; APS and EB-PVD are used in the production of TBCs. APS coatings grow as laminar while EB-PVD coatings grow as columnar [18]. Representations of coatings produced by APS and EB-PVD techniques are given in Fig. 1.

A splat-rich and porous structure is obtained through deposition on the substrate material by the PS coating method. Due to the high porosity content, the coatings produced by this method have a lower thermal conductivity. Columnar and granular structures are obtained in vertical direction on the substrate material through the EB-PVD method. In this coating method, porous structures form between the columns [19, 20]. Therefore, less porous structures compared to the PS method are obtained resulting in higher thermal conductivity values. However, since the TBCs produced with EB-PVD method allow higher expansion tolerances compared to those produced with the PS method, they exhibit a superior resistance [21].

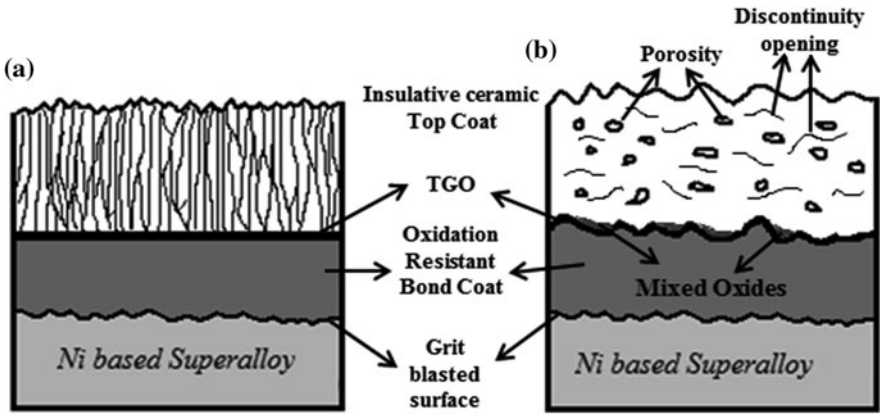

Fig. 1 TBC structures: **a** produced by EB-PVD method, **b** produced by APS method

2 Failure Mechanisms in TBCs

TBCs are exposed to various environmental effects causing occurrence of failures under service conditions. Failures occur as a result of one of these effects or combination of a number of effects. The main factors constituting the environmental effects occurring during service are: oxidation, hot corrosion, thermal shock/cycles, thermo-mechanic stresses, erosion and CMAS ($CaO–MgO–Al_2O_3–SiO_2$) failures [18]. The most effective failure mechanisms occurring as a result of mentioned failure factors include TGO-related failures such as the impairment of the integrity of TGO structure and TGO growth.

2.1 Oxidation

Since vibration and diffusion of the atoms are facilitated through temperature rise, diffusion of the oxygen is facilitated at high temperatures and accordingly the coating is oxidized at higher rates. Top YSZ coatings used in TBCs exhibit high oxygen permeability rates. Therefore, TGO formation is observed between the bond coat and top coat in TBCs. On the other hand bond coat production is also crucial in terms of oxidation resistance. The production of a porous bond coat similarly promotes TGO growth at high temperatures [16].

Since the oxidation increases in time, diffusion of aluminium towards the interface also increases due to its high affinity against oxygen, leading to the formation of a TGO having a higher aluminium thickness. In connection with the aluminium concentration within the coating, after a while aluminium will be completely oxidized and depleted resulting in mixed oxide formations. Due to the

mechanical properties of mixed oxide formations, local stresses will increase in the coating interface, resulting in a failure through spallation of the coating from the interface [22].

2.2 Hot Corrosion

Another failure caused by the top coating is hot corrosion. This type of failure occurs as a result of the infiltration of molten salts from the micro cracks at the top layer [23]. It forms under service conditions as a result of modifications in the structure of elements such as sodium, vanadium and lead. Such elements, emitted due to fuel pollution, react with the Y_2O_3 phase during their presence within the structure. In the absence of the Y_2O_3 phase, tetragonal-monoclinic phase transformation occurs due to improbability of the stabilization of the tetragonal ZrO_2 phase. This transformation may impair the integrity of the top layer through a modification in the volume [23]. In the latter case, this occurs due to the presence of phosphor and sodium caused by fuel pollution and through its reaction with zirconia. Occurrence of abovementioned corrosion mechanisms as a result of usage of low quality fuel or the service conditions impairs the integrity of the top coating and consequently result in the occurrence of failures [23, 24].

2.3 Thermal Shock

Thermal shock occurs via sudden temperature alteration whereas oxidation comes about chemical reactions at high temperatures. Thermal shock resistance is associated with various variables in the material. These are the thermal expansion coefficient, elastic module values, fracture resistance values of the material and the phase transformations occurring in the structure of some materials. The material group with the lowest resistance against thermal shock is the ceramics [25].

The top coating structure is desired to be compatible with the metallic bond coat to have a high thermal expansion coefficient and low elastic module, and exhibit a stable phase structure at high temperatures [26, 27]. Tensile stresses occur due to the thermal expansion growth coefficient mismatch between the substrate material and the top coat at high temperatures. During the heating process previously existing stresses are removed whereas compressive stresses occur following rapid cooling. Since the compressive stresses lead to further growth of the cracks, occurrence of failures in the coating will be observed over time.

There are three reasons for the spallation of the coating after thermal shock:

(i) Spallation failure resulting from the increase in stresses due to the growth of the oxide layer.
(ii) Expansions resulting from the thermal gradient within the oxide layer.

(iii) Mismatch between the thermal expansion coefficient of oxide layer and the coating [18, 28].

While tensile stresses occur in the oxide layer due to rapid heating, the tensile stresses forming between the coating and oxide interface result in deformation. As widely known, YSZ is the most preferred top ceramic coating material for TBC production. YSZ is subjected to a number of adverse effects following the loadings with thermal cycles. One is the decrease in the coating life due to increasing stresses as a result of limited expansion tolerance due to sintering effects, and the other is phase transformation of the t-tetragonal phase during coating life. At high temperatures t-tetragonal phase transforms into tetragonal and cubic phase, while during cooling it undergoes volumetric change and transforms into a monoclinic phase [18].

2.4 Thermo-Mechanical Failure

Formation mechanism of thermo-mechanical stresses vary based on the thermal condition to which the TBC is exposed. If the thermal condition is isothermal, then the mechanism is rather associated with TGO growth, whereas the mechanism for TBCs exposed to thermal cycle is associated with the shrinkage of TGO during cooling. It should be noted that both of these mechanisms may be effective, whereas one of them may be the dominant mechanism. For instance TBCs operating at high temperatures for long operating hours are used in the gas turbines used for energy production purposes. In this case isothermal mechanisms become effective and cooling-related expansion or shrinkage occurs when the turbine operation stops. As a result, in such turbines, limited number of thermal cycles and long duration isothermal heating occur and accordingly failure formation occurs as the TGO reaches an average thickness of 5–15 μm. In turbine components, TGO-related thermal expansion mismatch and TGO-growth-related failures become effective. However in the turbines used in aerospace industry in which the number of thermal cycles is the dominating factor, isothermal heating is not dominant, and failure occurs when the average TGO thickness is 1–5 μm, and this failure mainly arises from thermal cycles [11, 29].

2.5 $CaO–MgO–Al_2O_3–SiO_2$ (CMAS) Effect

CMAS is an environmental deposition form of the particles such as dust, rock, etc. and these type of particles frequently cause failure during service in applications related with the hot region components of the turbines. CMAS effect occurs as a result of melting of cations such as Ca, Mg, Al, Si TBCs at high temperatures. By interaction of CMAS and YSZ soda-silicate glass phase forms and it infiltrates into

TBC through open gaps. The CMAS effect in TBCs is closely related with the deposition methods. EB-PVD coatings are more vulnerable against CMAS attack due to their columnar microstructures. As a result of the thermal expansion difference between this phase and YSZ and the decrease in the expansion tolerance the cracks, thus the failure occurs [30–32].

2.6 Erosion Failure

TBCs are exposed to impurity and erosion failure after being exposed to particle impacts at burning tracks. Due to the vast number of micro cracks included by their microstructure, the TBCs are more susceptible to erosion failures compared to a highly dense ceramic structure. The erosion rate is higher in the TBCs compared to bulk ceramic materials. Additionally, TBC production methods are essential in terms of development of erosion failures in aerospace and industrial gas turbine engine components such as high pressure turbine blades [30, 33–35].

3 New Material Types in TBCs

The main purpose of TBCs is to decrease the heat conducted to the metallic substrate by use of a ceramic top coating with a low thermal conductivity. Mostly, ytrria stabilized zirconia (YSZ) is used as the top coating material for its superior mechanical, chemical and thermal characteristics [36–40].

In YSZ coatings, serious decreases may occur in the service life of YSZ coatings over 1200 °C by the effect of phase transformation and sintering [41–43]. Therefore, several studies are carried out for enhancement of YSZ and its service life. These are implemented through chemical modification of YSZ, use of a material with lower thermal conductivity or modifications in the microstructures [44–48].

The main characteristic expected from the ceramic top coatings that provide thermal insulation, is a low thermal conductivity. By use of a proper dopant, host atoms with varying valence numbers fill the gaps and cause the lattice to stretch. These two phenomena decrease the mean free path of scattered phonons, also decreasing the thermal conductivity. Zirconia based materials have low thermal conductivity. A more effective phonon dispersion is enabled through the formation of significant amounts of oxygen gaps by addition of a stabilizer, on the other hand transformation into monoclinic phase from tetragonal phase is prevented [49, 50]. For YSZ coating, if two or more dopants (instead of Y) add like rare earth elements, a lower thermal conductivity can be obtained due to more phonons scattering [51].

Oxides and zirconates of rare earth elements were found to have low thermal conductivity values [47, 52–54]. However, they have weak thermal cycle properties since their thermal expansion coefficients (CTE) are significantly lower compared

to metallic bond coats. This issue was resolved by the production of double layer coatings [47, 55, 56].

Even after a long period of use, $La_2Ce_2O_7$ does not exhibit a phase transformation at 1400 °C. Also having a high thermal expansion coefficient, $La_2Ce_2O_7$'s thermal cycle life increases after being coated with single and double ($La_2Ce_2O_7$/YSZ) layer [57–59]. Xuet al. observed that LZ/YSZ resisted a cycle 30 % longer than YSZ when they applied a thermal cycle test at 1373 K. LZ top coat was found to have undergone a significantly lower cycle failure compared to both [60].

ZrO_2—25 % CeO_2—2.5 % Y_2O_3 (CeSZ) produced by the EB-PVD method was observed to have a more stable phase structure with lower thermal conductivity and better corrosion resistance compared to YSZ. During the thermal cycle tests carried out a 1100 °C, TBCs with higher thermal cycle resistance and a longer service life, were obtained [61, 62].

At 700 °C, YSZ had a thermal conductivity value of 2.3 W/mK, while $Gd_2Zr_2O_7$, $Nd_2Zr_2O_7$ and $Sm_2Zr_2O_7$ had thermal conductivity values of 1.6, 1.6 and 1.5 W/mK, respectively [63]. The reason of the decline is the phonon dispersion caused by point flaws. These materials exhibit two types of point flaws. These are the oxygen gaps formed due to substitution of rare-earth cations with Zr and substitution of trivalent rare-earth elements with quadrivalent Zr. Dispersion intensity of the oxygen gaps is higher than the dispersion intensity of substitutional solid melts. Consequently the reason for having a lower conductivity compared to YSZ, is the higher oxygen gap concentration and a more effective phonon dispersion with dissolved cations due to the atomic mass difference between Zr and the cations [64].

A flawed cluster system is composed using more than one dopant. After addition of two cations one being smaller (as Yb, Sc) and one being larger (as Sm, Nd, Gd) to Y, a decrease in the thermal conductivity, compared to YSZ, was observed. Additionally, the total dopant concentration was also found to effect the conductivity. The TBCs produced by the PS method exhibited a decreased conductivity with 6–15 % molar addition, whereas lower thermal conductivity values were observed with 10 % molar addition in the TBCs produced by EB-PVD method. Multi-component oxide-based coatings were found to have a longer service life compared to YSZ after thermal cycle tests. Due to thermodynamically more stable and flawed lattice structure of added oxidized dopants, thermal conductivity decreased and sintering resistance increased [65, 66].

A significant decrease in the thermal conductivity values was obtained between 25 and 800 °C by addition of 6 wt% Niobia co-dopant to 8YSZ. The mean thermal conductivity value between 25 and 800 °C was measured as 1.171 W/mK for YSZ, whereas the mean value after Nb addition was measured as 0.542 W/mK [67].

Liu et al. [52] investigated the phase stability, sintering and thermal conductivity characteristics of 8 mol% Sc_2O_3, 0.6 mol% Y_2O_3 stabilized ZrO_2 (ScYSZ) prepared using a chemical co-precipitation method, and compared them with YSZ. The ScYSZ heated at 1500 °C for 300 h was found to be stable in $t^{'}$ phase, while the YSZ's 49.4 % was found to be in monolithic phase. The volume shrinkage of the samples reaches more than 26 % for 8YSZ whereas only 18 % for ScYSZ after heat treated up to

1500 °C. During the thermal conductivity measurements carried out between 30 and 700 °C ScYSZ was found to have a two times lower thermal conductivity compared to 8YSZ.

When the additions of NiO, Nd_2O_3, Gd_2O_3, Er_2O_3 and Yb_2O_3 oxides were examined, 4 % molar addition of all oxides except NiO resulted in a decrease in thermal conductivity. On the other hand addition of NiO resulted in a negligible decline in conductivity. Addition of 4 % mole of Er_2O_3 resulted in a 25 % decline, addition of 4 % mole of Nd_2O_3 resulted in a 42 % decline, while addition of Gd_2O_3 resulted in an average decline of 47 % in the conductivity. At each addition the crystal structure remained in tetragonal phase structure [68–70].

HfO_2, CeO_2 and ThO_2 TBCs constitute the oxide groups being used. CeO_2 is added to the system as Ce_2O_3 due to its volatility. Despite its adverse effect on sintering when compared with YSZ, it has the advantages of high thermal expansion coefficient and low thermal conductivity [71–73].

The minimum thermal conductivity value of HfO_2 doped YSZ is measured as 1.1 W m^{-1} K^{-1} at 1316 °C. Additionally, it was found to have a superior sintering resistance compared to YSZ [74].

As a magnetic ceramic material, lanthanium hexaluminate's ($LaMgAl_{11}O_9$) low thermal conductivity characteristic and low shrinkage characteristic renders it an alternative to YSZ. Most of La^{+3} cations are located on oxygen regions. Since the ion diffusion applies a vertical pressure to the c axis it has an inhibiting effect on sintering [75–77].

In Vassen et al.'s study [47] $SrZrO_3$, $BaZrO_3$, and $La_2Zr_2O_7$ powder's porosity content was reduced after being synthesised. Thermal expansion coefficients of $SrZrO_3$ and $BaZrO_3$'s were found to be lower than that of YSZ. $SrZrO_3$ did not prove to be a suitable TBC material since it underwent a phase transformation around 700–800 °C. Thermal conductivity of $La_2Zr_2O_7$ and $BaZrO_3$ sintered at 1000 °C are 1.6 and 3.4 W/mK respectively while YSZ has a thermal conductivity value of 2.2 W/mK. As for the hardness values, these two materials are observed two have a 15 % lower value compared to YSZ. Plasma sprayed $La_2Zr_2O_7$ was found to have a better thermal cycle life than $BaZrO_3$, but lower than YSZ.

4 Summary and Outlook

A wide range of current applications, production methods, failure mechanisms, and current uses of alternative materials in TBCs are reviewed in this study. High efficiency and performance increase constitute the main aspects of gas turbine engines during their development process. The increase in power and efficiency can be obtained only through increasing turbine inlet temperatures. The temperatures that the gas turbines are exposed to, are very close to or at the level of melting point of the super-alloy materials. Accordingly, complex cooling systems or TBCs are used as an attempt to protect super-alloy substrate materials against thermal failures and the adverse effects of hot gases.

Oxidation, hot corrosion effects, thermo-mechanical failures, chemical failures, erosion failures, sintering of top coating, thermal shock and CMAS (CaO-MgO-Al_2O_3-SiO_2) attack, constitute the primary failure mechanisms restricting the service life of TBCs. As a result of failure mechanisms arising from high temperature effects, thermal conductivity coefficient mismatches, changes in thermal conductivity coefficients as well as chemical interactions occur and as a result, TBCs undergo rapidly developing failures. A thorough analysis of these failure mechanisms that the TBCs undergo under service conditions, and implementation of failure prevention measures are essential in terms of providing a long-term and secure protection.

The efforts to increase the aimed turbine performance and efficiency for the new generation gas turbine engines necessitate higher turbine inlet temperatures as well as the development of TBC materials with long-term resistance against failures under such high temperatures. Thus, future investigations in TBCs with emphasis on surface engineering promise to reveal new high temperature materials and new insights in the years to come.

Acknowledgments This work was partially supported by The Scientific and Technological Research Council of Turkey (TUBITAK, 113R049).

References

1. Heveran CM, Xu JP, Sarin VK et al (2013) Simulation of stresses in TBC–EBC coating systems for ceramic components in gas turbines. Surf Coat Tech 235:354–360
2. Keyvani A, Saremi M, Sohi MH (2011) Oxidation resistance of YSZ-alumina composites compared to normal YSZ TBC coatings at 1100 °C. J Alloy Compd 509:8370–8377
3. Davis JR (1997) Protective coatings for superalloys, heat-resistance materials. ASM International, Ohio
4. Lu Z, Myoung SW, Kim EH et al (2014) Microstructure evolution and thermal durability with coating thickness in APS thermal barrier coatings. Mater Today: Proc 1:35–43
5. Pujol G, Ansart F, Bonino JP et al (2013) Step-by-step investigation of degradation mechanisms induced by CMAS attack on YSZ materials for TBC applications. Surf Coat Tech 237:71–78
6. Schulz U, Fritscher K, Leyens C (2000) Two-source jumping beam evaporation for advanced EB-PVD TBC systems. Surf Coat Tech 40:133–134
7. Padture NP, Gell M, Jordan EH (2002) Thermal barrier coatings for gas-turbine engine applications. Science 296:280–284
8. Bahadori E, Javadpour S, Shariat MH et al (2013) Preparation and properties of ceramic Al_2O_3 coating as TBCs on MCrAlY layer applied on Inconel alloy by cathodic plasma electrolytic deposition. Surf Coat Tech 228:611–614
9. Ma K, Schoenung JM (2011) Isothermal oxidation behavior of cryomilled NiCrAlY bond coat: homogeneity and growth rate of TGO. Surf Coat Tech 205:5178–5185
10. Evans HE (2011) Oxidation failure of TBC systems: an assessment of mechanisms. Surf Coat Tech 206:1512–1521
11. Evans AG, Mumm DR, Hutchinson JW et al (2001) Mechanisms controlling the durability of thermal barrier coatings. Prog Mater Sci 46:505–553

12. Taylor TA, Walsh PN (2004) Thermal expansion of MCrAlY alloys. Surf Coat Tech 177:24–31
13. Zhang Q, Li CJ, Li CX et al (2008) Study of oxidation behavior of nanostructured NiCrAlY bond coatings deposited by cold spraying. Surf Coat Tech 202:3378–3384
14. Richer P, Yandouzi M, Beauvais L et al (2010) Oxidation behaviour of CoNiCrAlY bond coats produced by plasma, HVOF and cold gas dynamic spraying. Surf Coat Tech 204:3962–3974
15. Su L, Zhang W, Sun Y et al (2014) Effect of TGO creep on top-coat cracking induced by cyclic displacement instability in a thermal barrier coating system. Surf Coat Tech 254:410–417
16. Chen WR, Wu X, Marple BR et al (2008) Pre-oxidation and TGO growth behaviour of an air-plasma-sprayed thermal barrier coating. Surf Coat Tech 202:3787–3796
17. Karaoglanli AC, Altuncu E, Ozdemir I et al (2011) Structure and durability evaluation of YSZ + Al_2O_3 composite TBCs with APS and HVOF bond coats under thermal cycling conditions. Surf Coat Tech 205:369–373
18. Karaoglanli AC, Ogawa K, Turk A et al (2013) Progress in gas turbine performance. Intech, Crotia
19. Peng H, Wang L, Guo L et al (2012) Degradation of EB-PVD thermal barrier coatings caused by CMAS deposits. Prog Nat Sci Mater Int 22:461–467
20. Rätzer-Scheibe HJ, Schulz U (2007) The effects of heat treatment and gas atmosphere on the thermal conductivity of APS and EB-PVD PYSZ thermal barrier coatings. Surf Coat Tech 201:7880–7888
21. Sampath S, Schulz U, Jarligo MO, Kuroda S (2012) Processing science of advanced thermal-barrier systems. MRS Bull Mater Res Soc 37:903–910
22. Xu H, Guo H (2011) Thermal barrier coatings. Woodhead Publishing, Cambridge
23. Saremi M, Afrasiabi A, Kobayashi A (2007) Bond coat oxidation and hot corrosion behavior of plasma sprayed YSZ coating on Ni superalloy Trans JWRI 36:41–45
24. Jones RL (1997) Some aspects of the hot corrosion of thermal barrier coatings. J Therm Spray Technol 6:77–84
25. Ghosh S (2014) Thermal behavior of glass–ceramic bond coat in a TBC system. Vacuum 101:367–370
26. Karger M, Vaßen R, Stöver D (2011) Atmospheric plasma sprayed thermal barrier coatings with high segmentation crack densities: spraying process, microstructure and thermal cycling behavior. Surf Coat Tech 206:16–23
27. Guo HB, Vaßen R, Stöver D (2004) Atmospheric plasma sprayed thick thermal barrier coatings with high segmentation crack density. Surf Coat Tech 186:353–363
28. Sun J, Fu QG, Liu GN et al (2015) Thermal shock resistance of thermal barrier coatings for nickel-based superalloy by supersonic plasma spraying. Ceram Int 41:9972–9979
29. Wright PK, Evans AG (1999) Mechanisms governing the performance of thermal barrier coatings. Curr Opin Solid St M 4:255–265
30. Aygun A (2008) Novel Thermal Barrier Coatings (TBCs) that are resistant to high temperature attack by CaO-MgO-Al_2O_3-SiO_2 (CMAS) glassy deposits, PhD thesis, The Ohio State University
31. Steinke T, Sebold D, Mack DE et al (2010) A novel test approach for plasma-sprayed coatings tested simultaneously under CMAS and thermal gradient cycling conditions. Surf Coat Tech 2057:2287–2295
32. Li L, Hitchman N, Knapp J (2010) Failure of thermal barrier coatings subjected to CMAS attack. J Therm Spray Technol 19:148–155
33. Clarke DR, Levi CG (2003) Materials design for the next generation thermal barrier coating. Ann Rev Mater Res 33:383–417
34. Strangman T, Raybould D, Jameel A et al (2007) Damage mechanisms, life prediction, and development of EB-PVD thermal barrier coatings for turbine airfoils. Surf Coat Tech 202:658–664

35. Nicholls JR, Deakinand MJ, Rickerby DS (1999) A Comparison between the erosion behaviour of thermal spray and electron physical beam vapour deposition thermal barrier coatings. Wear 352:233–235
36. Bose S, Demasi J (1997) Thermal barrier coating experience in gas turbine engines. J Therm Spray Technol 6:99–104
37. Han M, Zhou G, Huang J, Chen S (2014) Optimization selection of the thermal conductivity of the top ceramic layer in the double-ceramic-layer thermal barrier coatings based on the finite element analysis of thermal insulation. Surf Coat Tech 240:320–326
38. Hass DD, Slifka AJ, Wadley HNG (2001) Low thermal conductivity vapor deposited zirconia microstructures. Acta Mater 49:973–983
39. Ferdinando MD, Fossati A, Lavacchi A et al (2010) Isothermal oxidation resistance comparison between air plasma sprayed, vacuum plasma sprayed and high velocity oxygen fuel sprayed CoNiCrAlY bond coats. Surf Coat Tech 204:2499–2503
40. Richer P, Yandouzi M, Beauvais L et al (2010) Oxidation behaviour of CoNiCrAlY bond coats produced by plasma, HVOF and cold gas dynamic spraying. Surf Coat Tech 204:3962–3974
41. Ma W, Jarligo MO, Mack DE, Pitzer D et al (2008) New generation perovskite thermal barrier coating materials. J Therm Spray Technol 17:5–6
42. Clarke DR, Levi CG (2003) Materials design for the next generation thermal barrier coatings. Ann Rev Mater Res 33:383–417
43. Habibi MH, Wang L, Liang J et al (2013) An investigation on hot corrosion behavior of YSZ-Ta2O5 in Na2SO4 + V2O5 salt at 1100 °C. Corr Sci 75:409–414
44. Nicholls JR (2003) Advances in coating design for high-performance gas turbines. MRS Bull 28:659–670
45. Levi CG (2004) Emerging materials and processes for thermal barrier systems. Curr Opin Solid State Mater Sci 8(1):77–91
46. Ning XJ, Li CX, Li CJ, Yang GJ (2006) Modification of microstructure and electrical conductivity of plasma-sprayed YSZ deposit through postdensification process. Mater Sci Eng 428(1–2):98–105
47. Vassen R, Cao X, Tietz F, Basu D, Stöver D (1999) Zirconates as new materials for thermal barrier coatings. J Am Ceram Soc 83:2023–2028
48. Stöver D, Funke C (1999) Directions of the development of thermal barrier coatings in energy applications. J Mater Process Tech 195:92–93
49. Schulz U, Fritscher K, Leyens C (2000) Two-source jumping beam evaporation for advanced EB-PVD system. Surf Coat Tech 40:133–134
50. Guo X, Wang Z (1998) Effect of niobia on the defect structure of yttria-stabilized zirconia. J Euro Ceram Soc 18:237–240
51. Xu H, Wu J (2011) Thermal barrier coatings. Woodhead Publishing, Cambridge
52. Liu H, Li S, Li Q et al (2010) Investigation on the phase stability, sintering and thermal conductivity of Sc_2O_3–Y_2O_3–ZrO_2 for thermal barrier coating application. Mater Design 31:2972–2977
53. Suresh G, Seenivasan G, Krishnaiah MV, Murti PS (1997) Investigation of the thermal conductivity of selected compounds of gadolinium and lanthanum. J Nucl Mater 249:259–261
54. Saruhan B, Francois P, Kritscher K et al (2004) EB-PVD processing of pyrochlore-structured $La_2Zr_2O_7$-based TBCs. Surf Coat Tech 182:175–183
55. Stöver D, Pracht G, Lehmann H et al (2004) New material concepts for the next generation of plasma-sprayed thermal barrier coatings. J Therm Spray Technol 13:76–83
56. Vassen R, Traeger F, Stöver D (2004) New thermal barrier coatings based on pyrochlore/YSZ double layer systems. Int J Appl Ceram Techl 1:351–356
57. Cao X, Vassen R, Fischer W et al (2003) Lanthanum-cerium oxide as a thermal barrier-coating material for high-temperature applications. Adv Mater 15:1438–1442
58. Ma W, Gong SK, Xu HB et al (2006) On improving the phase stability and thermal expansion coefficients of lanthanum cerium oxide solid solutions. Scripta Mater 54:1505–1508

59. Ma W, Gong SK, Xu HB et al (2006) The thermal cycling behavior of lanthanum-cerium oxide thermal barrier coating prepared by EB–PVD. Surf Coat Tech 200:5113–5118
60. Xu Z, He L, Mu R et al (2009) Double-ceramic-layer thermal barrier coatings of $La_2Zr_2O_7$/YSZ deposited by electron beam-physical vapor deposition. J Alloy Compd 473:509–515
61. Schulz U, Fritscher K, Peters M (1996) EB-PVD Y_2O_3- and $CeO_2Y_2O_3$-stabilized zirconia thermal barrier coatings—crystal habit and phase composition. Surf Coat Tech 82:259–269
62. Leyens C, Schulz U, Fritscher K (2003) Oxidation and lifetime of PYSZ and CeSZ coated Ni-base substrates with MCrAlY bond layers. Mater High Temp 20:475–480
63. Wu J, Wei X, Padture NP et al (2002) Low thermal conductivity rare-earth zirconates for possible thermal-barrier coatings application. J Am Ceram Soc 85:3031–3035
64. Lee KN (2006) In the gas turbine handbook. NETL, Cleveland
65. Zhu DM, Miller RA (2002) In: Lin HT, Singht M (eds) Thermal conductivity and sintering behavior of advanced thermal barrier coatings, 4th edn. The American Ceramic Society, Florida
66. Zhu DM, Chen YL, Miller RA (2003) Defect clustering and nano-phase structure characterization of multi-component rare earth oxide doped zirconia-yttria thermal barrier coatings. Ceram Eng Sci Proc 24:525–534
67. Almeida DS, Silva CRM, Nono MCA et al (2007) Thermal conductivity investigation of zirconia co-doped with yttria and niobia EB-PVD TBCs. Mater Sci Eng, A 443:60–65
68. Tamarin YA, Kachanov EB, Zherzdev SV (1997) Thermophysical properties of ceramic layers in TBC-EB. Mater Sci Forum 251–254:949–956
69. Nicholls JR, Lawson KJ, Johnstone A et al (2001) Low thermal conductivity EB-PVD thermal barrier coatings. Mater Sci Forum 369:595–606
70. Nicholls JR, Lawson KJ, Johnstone A et al (2002) Methods to reduce the thermal conductivity of EB-PVD TBCs. Surf Coat Tech 151–152:383–391
71. Gao W, Li Z (2008) Developments in high temperature corrosion and protection of materials. Woodhead Publishing, Cambridge
72. Thornton J, Majumdar A, Mcadam G (1997) Enhanced cerium migration in ceria-stabilised zirconia. Surf Coat Tech 94(95):112–117
73. Agarwal AK, Pandey A, Gupta AK et al (2014) Novel combustion concepts for sustainable energy development. Springer, India
74. Singh J, Wolfe DE, Miller RA et al (2004) Tailored Microstructure of zirconia and hafnia-based thermal barrier coatings with low thermal conductivity and high hemispherical reflectance by EB-PVD. J Mater Sci 39:1975–1985
75. Gadow R, Lischka M (2002) Lanthanum hexaaluminate—novel thermal barrier coatings for gas turbine applications—materials and process development. Surf Coat Tech 151:392–399
76. Cao XQ, Vassen R, Stöver D (2004) Ceramic materials for thermal barrier coatings. J Euro Ceram Soc 24:1–10
77. Cao XQ, Zhang YF, Zhang JF (2008) Failure of the plasma-sprayed coating of lanthanum hexaluminate. J Euro Ceram Soc 28:1979–1986